PLANT SCIENCE TODAY
ISSN 2348-1900 (online)
Vol 11(1): 531–543
https://doi.org/10.14719/pst.3016

HORIZON
e-Publishing Group
HePG

RESEARCH ARTICLE

In silico screening of phytoconstituents of *Cissus quadrangularis* and *Chromolaena odorata* against proteins of antimicrobial resistance and wound healing

Aparna S. Sivapria, Bibu John Kariyil*, Priyanka Menon K & Hari Sankar V. J

Department of Veterinary Pharmacology and Toxicology, College of Veterinary and Animal Sciences, Kerala Veterinary and Animal Sciences University, Thrissur 680651, India

*Email: bibujohn@kvasu.ac.in

OPEN ACCESS

ARTICLE HISTORY

Received: 13 November 2023
Accepted: 30 November 2023

Available online
Version 1.0 : 10 January 2024
Version 2.0 : 24 January 2024

Check for updates

Additional information

Peer review: Publisher thanks Sectional Editor and the other anonymous reviewers for their contribution to the peer review of this work.

Reprints & permissions information is available at https://horizonepublishing.com/journals/index.php/PST/open_access_policy

Publisher's Note: Horizon e-Publishing Group remains neutral with regard to jurisdictional claims in published maps and institutional affiliations.

Indexing: Plant Science Today, published by Horizon e-Publishing Group, is covered by Scopus, Web of Science, BIOSIS Previews, Clarivate Analytics, NAAS, UGC Care, etc
See https://horizonepublishing.com/journals/index.php/PST/indexing_abstracting

CITE THIS ARTICLE

Aparna S S, Bibu J K, Priyanka M K, Hari S V. J. *In silico* screening of phytoconstituents of *Cissus quadrangularis* and *Chromolaena odorata* against proteins of antimicrobial resistance and wound healing . Plant Science Today. 2024; 11(1): 531–543. https://doi.org/10.14719/pst.3016

Abstract

In silico screening is a methodological approach, which is invaluable for rational drug design and the identification of potential therapeutic agents. In the context of antibiotic-resistant infectious wounds, molecular docking can provide a deeper understanding of how phytocompounds might interfere with bacterial virulence and antibiotic resistance. In this study, proteins involved in antimicrobial resistance and wound healing were docked against major phytoconstituents of ethyl acetate extract of *Cissus quadrangularis* (EACQ) and ethanol extract of *Chromolaena odorata* (EECO), two medicinal plants that have been traditionally used. Receptor structures for interleukin 6 (PDB id: 1n26) IL6, of human and mice, IL6 (Uniprot id p 20607) of rat, vascular endothelial growth factor (VEGFR, PDB id: 2ctw) for human, mice, rat and penicillin binding protein 2a (PBP2a, PDB id: 1vqq) of *S. aureus* were downloaded from the database of the RCSB protein data bank. The ligand structures were downloaded from PubChem compound database in structure data file (.SDF) format. The docking studies were conducted using Autodock4. and the results of the docking analysis were visualised using Discovery Studio Visualizer. The docking log (dlg) file, featuring an RMSD table, provides binding energy values in Kcal/mol for each molecule at its optimal docked postures, offering insights into structural accuracy and ligand-receptor interaction strength in molecular docking simulations. *In silico* analysis of ligands showed that squalene of EACQ and epilupeol of EECO had the least binding energy towards proteins of antimicrobial resistance and wound healing. Thus, these compounds could emerge as promising lead molecules against infectious wounds.

Keywords

Cissus quadrangularis; *Chromolaena odorata*; ethnopharmacology; infectious wounds; molecular docking wound healing

Introduction

Wound healing, as a normal biological process in the human body, is achieved through four precisely and highly programmed phases: hemostasis, inflammation, proliferation, and remodelling. For a wound to heal successfully, all four phases must occur in the proper sequence and time frame (1). However, the emergence and spread of antibiotic-resistant bacteria, especially methicillin-resistant *Staphylococcus aureus* (MRSA) have posed significant challenges to successful wound healing. Integration of a staphylococcal cassette chromosome *mec* (SCC*mec*) element into the chro-

mosome converts drug-sensitive *S. aureus* into the notorious hospital pathogen MRSA, which is resistant to practically all β-lactam antibiotics (2). In recent years, the search for alternative therapeutic approaches has intensified, with a focus on natural products and traditional remedies with potential wound healing properties. *Cissus quadrangularis* and *Chromolaena odorata* are two medicinal plants that have been traditionally used in various cultures for their purported wound healing effects.

C. quadrangularis (L.) commonly known as "Hadjod" or "Veldt Grape," belongs to the Vitaceae family and is native to tropical regions of Asia and Africa. It has been employed in traditional medicine for its anti-inflammatory, analgesic, and bone-regenerating properties (3). Similarly, *C. odorata*, (L.) King and Rob. also known as "Siam Weed" or "Jack-in-the-Bush," is a plant native to Central and South America. It has a long history of use in traditional medicine as an antimicrobial and wound healing agent (4).

Given the widespread use of these two plant extracts in traditional medicine, there is a growing interest in evaluating their wound healing potential, particularly in the context of antibiotic-resistant infectious wounds. Thus, this study aims to investigate the antibiotic-resistant infectious wound healing activity of phytoconstituents detected in *C. quadrangularis* and *C. odorata* extracts using molecular docking.

Molecular docking is a computational technique that enables us to simulate and predict the binding interactions between molecules at the atomic level. In our context, it offers a powerful tool for elucidating the potential interactions between phytocompounds and MRSA-associated molecular targets, such as enzymes and proteins. By virtually "docking" these compounds into the target structures, we can gain insights into their binding affinity, binding modes, and the strength of their interactions.

This methodological approach is invaluable for rational drug design and the identification of potential therapeutic agents. In the context of antibiotic-resistant infectious wounds, molecular docking can provide a deeper understanding of how phytocompounds might interfere with bacterial mechanisms of virulence and antibiotic resistance. Moreover, it can help us to pinpoint the most promising candidates for further experimental validation.

This research will contribute to the growing body of knowledge on natural products and their potential therapeutic benefits in wound healing, especially in the context of antibiotic-resistant infections. The findings from this study may pave the way for the development of novel and effective treatments that can complement or even replace conventional therapies for antibiotic-resistant infectious wounds, thereby offering new hope for patients facing challenging wound healing scenarios. Ultimately, the exploration of these traditional remedies holds promising prospects for enhancing wound management strategies and improving patient outcomes in the face of antibiotic resistance.

Materials and Methods

Preparation of extracts

C. quadrangularis and *C. odorata* were collected, shade-dried and extracted using ethyl acetate as solvent for *C. quadrangularis* (EACQ) and ethanol as solvent for *C. odorata* (EECO). The EACQ and EECO are reported to have antimicrobial activity against *S. aureus* (5,6). These extracts were used for gas chromatography-mass spectroscopy analysis.

Gas chromatography mass spectroscopy

Gas chromatography-mass spectroscopy analysis of extracts was done at Kerala Forests Research Institute, Peechi, Kerala, India. Gas chromatography Mass Spectrometer (Shimadzu Nexis GC- 2030) with a mass range of 1.5- 1000 m/z was used. Helium was used as the carrier gas at flow rate of 1 mL/min. The oven temperature was maintained at 60° C and then increased to 280° C in 5 min. The injector temperature was 260° C and total analysis time was 50 min. Aliquots of extracts (0.4 µL) were injected into the chromatographic column after a clear baseline was obtained. Major constituents were identified by using mass spectrum library (NIST 20).

Preparation of macromolecule

Receptor structures for interleukin 6 (PDB id: 1n26) IL6, of human and mice, IL6 (Uniprot id p 20607) of rat, vascular endothelial growth factor (VEGFR, PDB id: 2ctw) of human, mice, rat and penicillin binding protein 2a (PBP2a) (PDB id: 1vqq) (Fig. 1) were downloaded from the database of the RCSB protein data bank (http://www.rcsb.org) in PDB format. The structure was prepared using Accelrys Discovery Studio Visualizer 3.5.0.12158 (Copyright© 2005-12, Biovia Software Inc) for further processing and docking. Further, the macromolecule was processed in AutoDock 1.5.6 (Molecular Graphics Laboratory tools, www.mgltools.scripps.edu) according to the AutoDock Tools (ADT) tutorial's standard protocol and parameters.

Preparation of ligand

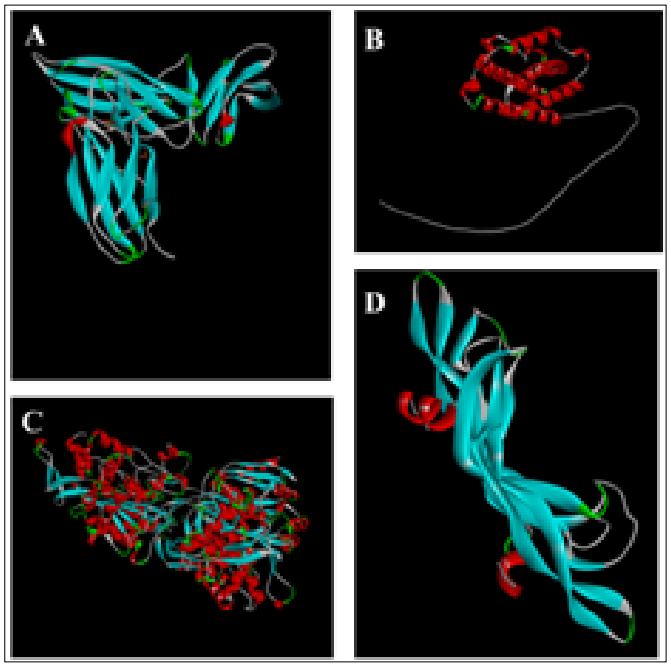

Fig. 1: Structure of receptor proteins. **A**- IL 6 (human and mice, PDB ID- 1N26), **B**-IL 6 (rat, UNIPROT ID- P20607), **C**- VEGFR (human, rat and mice, PDB ID- 2C7W), **D**- PBP 2a (human, rat and mice, PDB ID- 1VQQ)

Phytoconstituents of *C. quadrangularis* and *C. odorata* obtained by GC-MS were the ligands used in this study. Indomethacin, allantoin and ceftriaxone were used as the standards (Fig. 2). The ligand structures (Fig. 3 and 4) were downloaded from PubChem compound database (National Center for Biotechnology Information; https://pubchem ncbi.nlm.nih.gov/) in structure data file (.SDF) format. Then they were processed using Marvin View 17.25.0 (www.chemaxon.com) and modified to Tripos Mol 2 format. The modifying tools of ADT for ligands were used for processing them in terms of detection of roots, root expansion and choosing the number of rotatable bonds. Following the preliminary preparations, the ligand molecules were transformed to PDBQT format for use in AutoDock4.

Methodology of docking

The docking studies were conducted using Autodock4 developed by the Scripps Research Institute (La Jolla, CA, www.autodock.scripps.edu). The grid map for the present study was computed with Autodock4. The grid centre was set as tabulated (Table 1). The processed file was saved in grid parameter file (gpf) format. Using the parameters optimised by ADT, the docking parameter file (dpf) was generated. The Lamarckian genetic algorithm was used for all docking runs. The docking log (dlg) file with RMSD table contained the binding energy (KCal/mol) for each molecule's optimal docked postures.

Visualisation of results

Table 1. Grid parameters set for different proteins

PROTEIN	X	Y	Z
1N26	20.2461	59.2435	90.3015
P20607	4.73822	1.35322	12.1825
2C7W	37.6230	48.1946	12.8574
1VQQ	5.1627	36.8798	47.8622

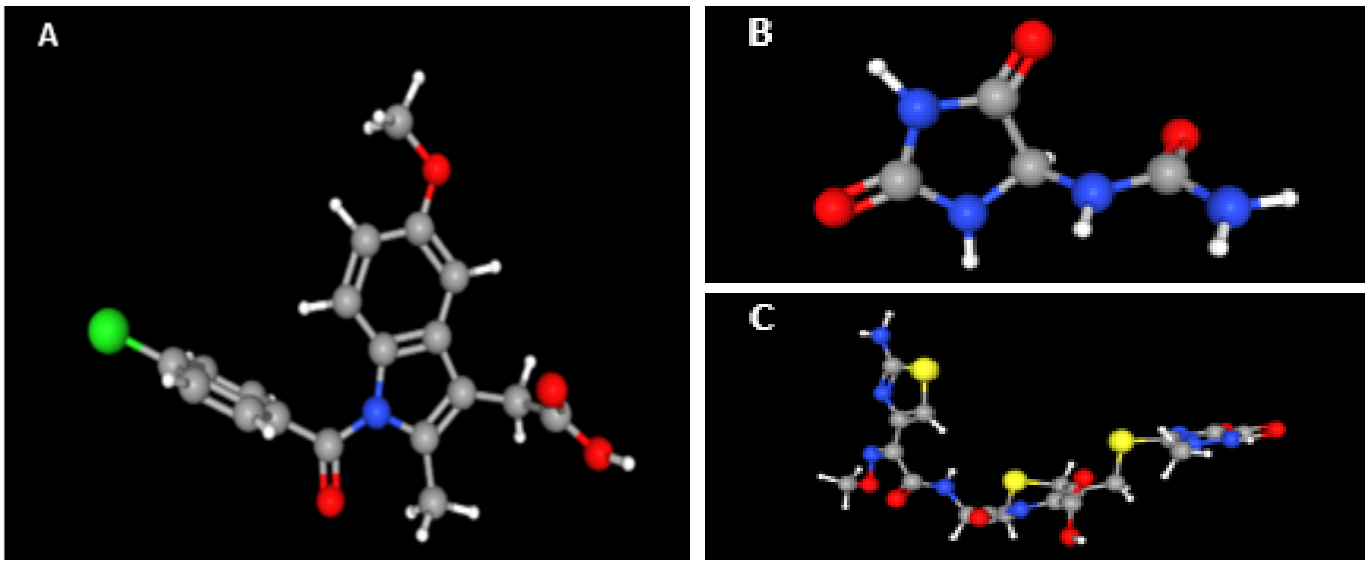

Fig. 2: Standards used: **A**- indomethacin, **B**- allantoin, **C**- ceftriaxone

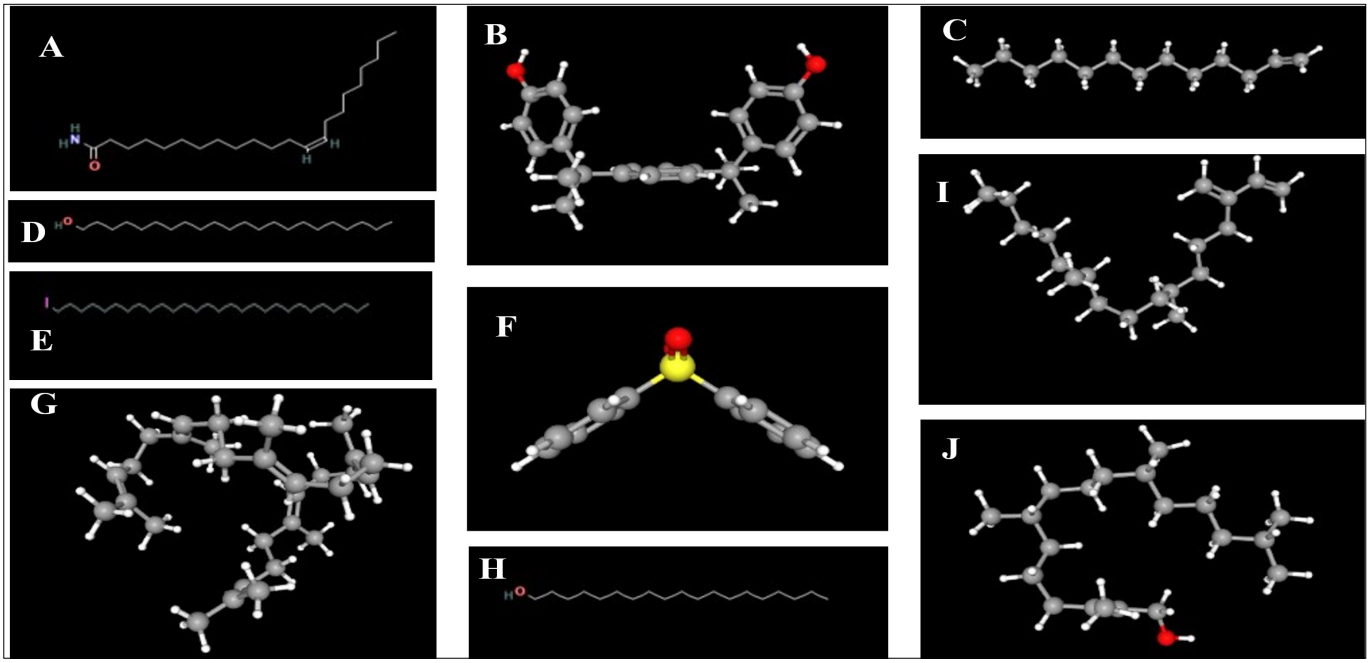

Fig. 3- Phytocompounds of *Cissus quadrangularis:* **A**- (Z)-13-Docosenamide, **B**- 4,4'-((p- Phenylene) diisopropylidene) diphenol, **C**- 1-Tridecene, **D**- Behenic alcohol, **E**- 1-iodo-Octacosane, **F**- Diphenyl sulfone, **G**- Squalene, **H**- n-Nonadecanol-1, **I**- Neophytadiene, **J**- Phytol

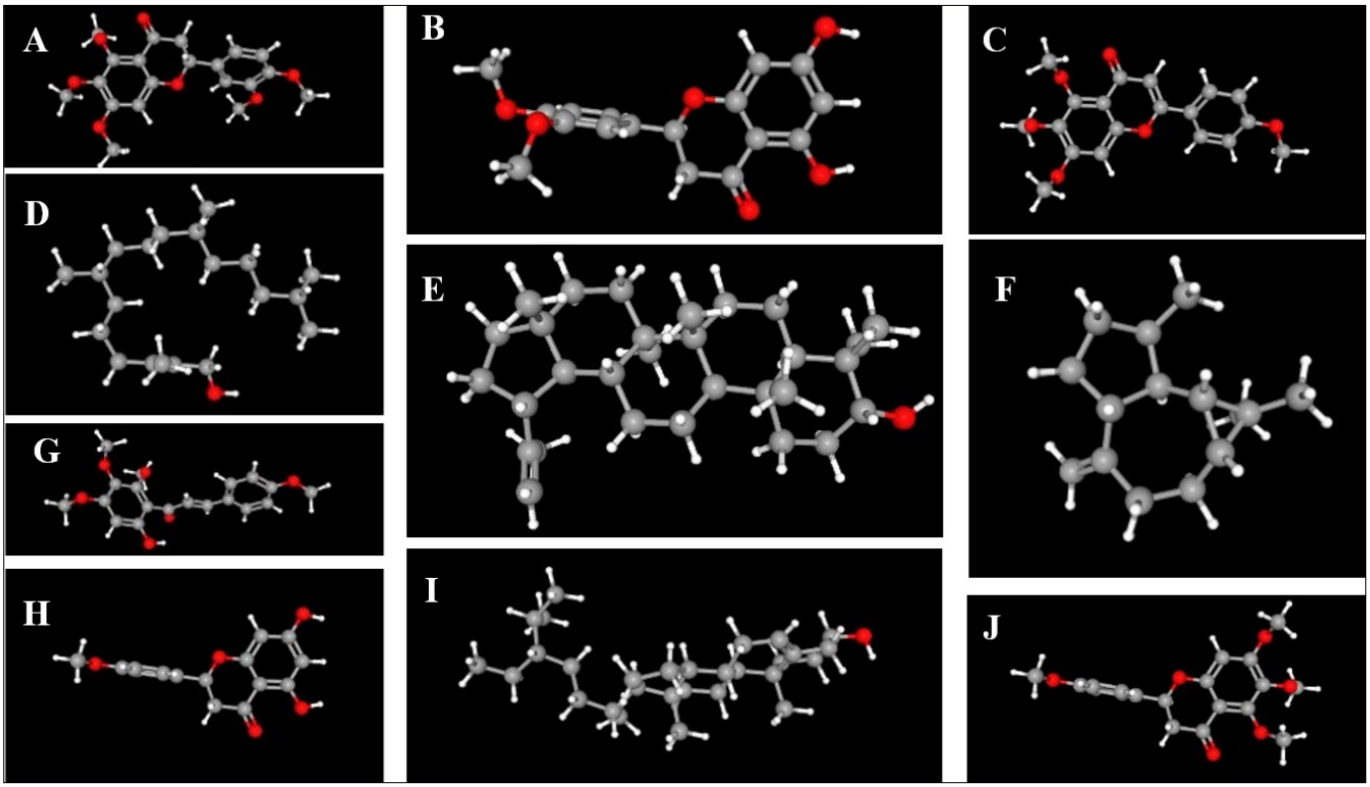

Fig. 4- Phytocompounds of *Chromolaena odorata* :**A**- 3',4',5,6,7-Pentamethoxyflavanone, **B**- 2-(3,4-Dimethyloxyphenyl)-2,3-dihydro-5,7-dihydroxy-4H-1-benzopyran-4-one, **C**- 4H-1-Benzopyran-4-one, 5,6,7-trimethoxy-2-(4-methoxyphenyl), **D**- Phytol, **E**- Epilupeol, **F**- Aromandendrene, **G**- 2'-Hydroxy-4,4',5',6'-tetramethoxychalcone, **H**- Isosakuranetin, diacetate, **I**- gamma-Sitosterol, **J**- 5,6,7,4'-Tetramethoxyflavanone

Using Discovery Studio, the results of the docking analysis were visualised. After studying each ligand interactions with the protein and analysing their binding poses, the best and most energetically beneficial conformations of each ligand were selected (Laskowski and Swindells, 2011).

Results

GC- MS analysis of EACQ and EECO

Chromatograms obtained for EACQ (Figure 5) and EECO (Figure 6) on are given. The compounds obtained on GC-MS analysis of EACQ (Table 2) and EECO (Table 3) are listed. Gas chromatography- mass spectroscopic analysis

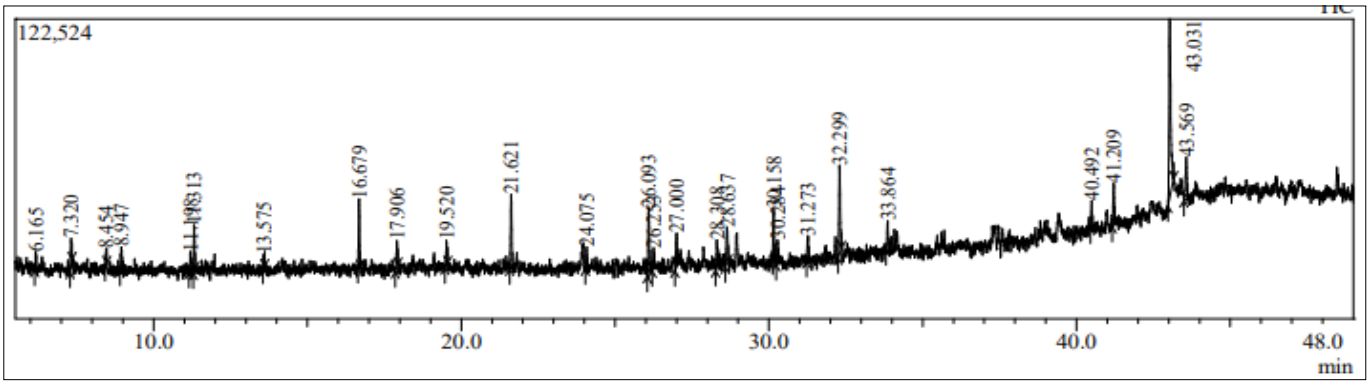

Fig.5. Chromatogram of EACQ

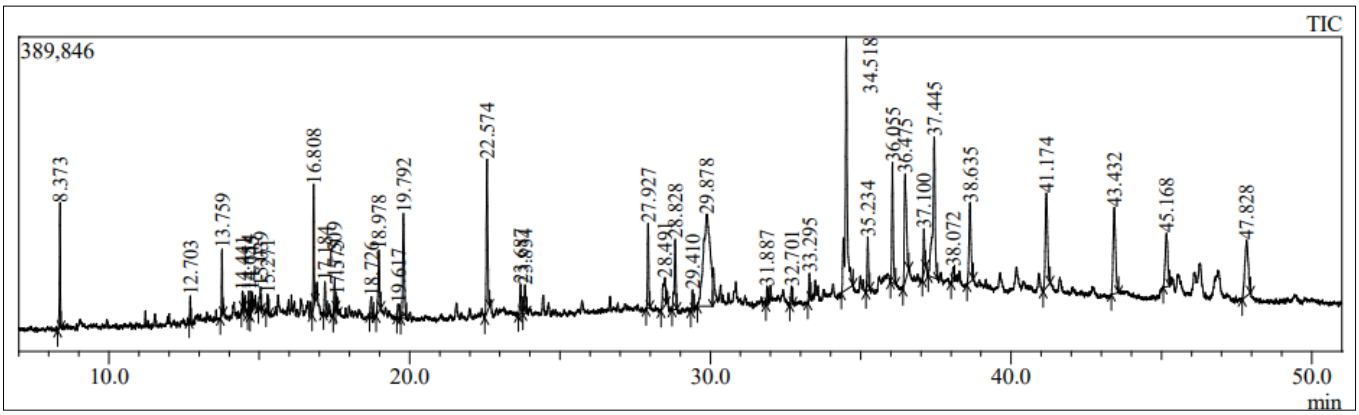

Fig.6. Chromatogram of EECO

Table 2. Phytochemicals obtained on GC- MS analysis of EACQ stem

Sl. No.	Compound name	Retention time	Area percentage
1.	1-Decene	6.165	0.99
2.	2-Pyrrolidinone, 1-methyl-	7.320	1.59
3.	Benzaldehyde, 4-methyl-	8.454	0.83
4.	Nonanal	8.947	2.05
5.	1-Tridecene	11.313	3.45
6.	Dodecane, 4,6-dimethyl-	13.575	0.70
7.	1-Tetradecene	16.679	5.10
8.	Quinoline, 1,2-dihydro-2,2,4-trimethy	17.906	2.19
9.	2,4-Di-tert-butylphenol	19.520	1.71
10.	1-Hexadecanol	21.621	6.47
11.	Heneicosane	24.075	1.82
12.	n-Nonadecanol-1	26.093	5.62
13.	Octacosane, 1-iodo-	26.253	1.67
14.	Neophytadiene	27.000	3.51
15.	Heneicosane	28.308	2.58
16.	Diphenyl sulfone	28.637	4.12
17.	Behenic alcohol	30.158	4.01
18.	Eicosane	30.284	1.87
19.	Cyclic octaatomic sulfur	31.273	2.77
20.	Phytol	32.299	8.27
21.	1-Heptacosanol	33.864	2.71
22.	Tetrapentacontane	40.492	2.19
23.	13-Docosenamide, (Z)-	43.031	23.24
24.	Squalene	43.569	5.09

of EACQ revealed the presence of 1-decene, 1-methyl-2-

Table 3. Phytochemicals obtained on GC- MS analysis of EECO leaves

Sl.No.	Name	Retention time	Area per cent
1.	7,9-Di-tertbutyl-1-oxaspiro[4,5]deca-6,9-dien-8-one	12.703	0.42
2.	9-Methyl-10-methylenetricyclo[4.2.1.1(2,5)]decan-9-ol	13.759	1.14
3.	Benzoic acid, 4-hydroxy-3-methoxy-, ethyl ester	14.441	0.28
4.	Isolongifolol	14.654	0.43
5.	S-(p-Methoxybenzoyl)thiohydroxylamine	14.745	0.36
6.	Sulfurous acid, cyclohexylmethyl octadecyl ester	15.039	0.57
7.	2,5-Cyclohexadiene-1,4-dione, 2-hydroxy-3,5,6-trimethyl-	15.271	0.50
8.	Neophytadiene	16.808	2.65
9.	Isophthalic acid, 3,7-dimethyloct-6-enyl tridecyl ester	17.184	0.98
10.	Neophytadiene	17.509	0.80
11.	2,4'-Dihydroxy-3'-methoxyacetophenone	17.575	0.32
12.	Benzothiazole, 2-(2-hydroxyethylthio)-	18.726	0.66
13.	n-Hexadecanoic acid	18.978	2.05
14.	2H-Pyran-2-one, tetrahydro-6-octyl-	19.617	0.54
15.	Hexadecanoic acid, ethyl ester	19.792	3.81
16.	Phytol	22.574	4.95

17.	trans,trans-9,12-Octadecadienoic acid, propyl ester	23.687	0.98
18.	Ethyl Oleate	23.834	0.95
19.	(-)-Neoclovene-(I), dihydro-	27.927	2.30
20.	(.+/-.)-.beta.-Isocomene	28.491	1.64
21.	Aromandendrene	28.828	2.47
22.	4-Acetyloxy-8-(3-oxo-2-pent-2-enylcyclopenten-1-yl)octanoic acid	29.410	0.58
23.	.gamma.-Sitosterol	29.878	14.30
24.	Docosanoic acid, ethyl ester	31.887	0.51
25.	5-Hydroxy-4',7-dimethoxyflavanone	33.295	0.69
26.	Isosakuranetin, diacetate	34.518	11.67
27.	Squalene	35.234	1.48
28.	5,6,7,4'-Tetramethoxyflavanone	36.055	3.75
29.	2-(3,4-Dimethyloxyphenyl)-2,3-dihydro-5,7-dihydroxy-4H-1-benzopyran-4-on	36.475	5.15
30.	2-Propen-1-one, 3-(4-hydroxyphenyl)-1-(2-hydroxy-3,4,6-trimethoxyphenyl)-	37.100	1.30
31.	2'-Hydroxy-4,4',5',6'-tetramethoxychalcone	37.445	7.58
32.	Docosanoic acid, ethyl ester	38.072	0.50
33.	3',4',5,6,7-Pentamethoxyflavanone	38.635	3.62
34.	4H-1-Benzopyran-4-one, 5,6,7-trimethoxy-2-(4-methoxyphenyl)-	41.174	4.81
35.	Stigmasterol	43.432	4.90
36.	.gamma.-Sitosterol	45.168	3.15
37.	Epilupeol	47.828	4.33

pyrrolidinone, 4-methyl-benzaldehyde, nonanal, 1-tridecene, 4,6-dimethyl-dodecane, 1-tetradecene, 1,2-dihydro-2,2,4-trimethyl quinoline, 2,4-di-tertbutyl-phenol, 1-hexadecanol, heneicosane, n-nonadecanol-1, 1-iodo-octacosane, neophytadiene, heneicosane, diphenyl sulfone, behenic alcohol, eicosane, cyclic octaatomic sulfur, phytol, 1-heptacosanol, tetrapentacontane, (Z)-13-docosenamide and squalene.

Gas chromatography- mass spectrometric analysis of EECO showed the presence of active ingredients such as isolongifolol, s-(p-methoxybenzoyl)thiohydroxylamine, sulfurous acid, cyclohexylmethyl octadecyl ester, neophytadiene, isophthalic acid, 3,7-dimethyloct-6-enyl tridecyl ester, neophytadiene, hexadecanoic acid, ethyl ester, phytol, trans,trans-9,12-octadecadienoic acid, propyl ester, ethyl oleate, dihydro- (-)-neoclovene-(I), (.+/-.)-.beta.-isocomene, aromandendrene, 4-acetyloxy-8-(3-oxo-2-pent-2-enylcyclopenten-1-yl) octanoic acid, gamma sitosterol, docosanoic acid, ethyl ester, 4, 5-hydroxy-4',7-dimethoxyflavanone, isosakuranetin diacetate, squalene, 5,6,7,4'-tetramethoxyflavanone, 2-(3,4-dimethyloxyphenyl)-2,3-dihydro-5,7-dihydroxy-4H-1-benzopyran-4-on, 3-(4-hydroxyphenyl)-1-(2-hydroxy-3,4,6-trimethoxyphenyl)-2-propen-1-one, 2'-hydroxy-4,4',5',6'-tetramethoxychalcone, ethyl ester docosanoic acid, 3',4',5,6,7-pentamethoxy-flavanone, 5,6,7-trimethoxy-2-(4-methoxyphenyl)-4H-1-benzopyran-4-one, stigmasterol, gamma- sitosterol and epilupeol. From these compounds, peaks with higher area percentage in the chromatogram were selected for *in silico* analysis (Table 4).

Table 4. Different ligands selected for *in silico* analysis

C. quadrangularis	***C. odorata***
1-Tridecene	gamma-Sitosterol
(Z)-13-Docosenamide	2-(3,4-Dimethyloxyphenyl)-2,3-dihydro-5,7-dihydroxy-4H-1-benzopyran-4-one
Behenic alcohol	2'-Hydroxy-4,4',5',6'-tetramethoxychalcone
Diphenyl sulfone	3',4',5,6,7-Pentamethoxyflavanone
NeophytadieneS	4H-1-Benzopyran-4-one, 5,6,7-trimethoxy-2-(4-methoxyphenyl)-
n-Nonadecanol-1	5,6,7,4'-Tetramethoxyflavanone
1-iodoOctacosane,	Aromandendrene
Phytol	Epilupeol
Squalene	Isosakuranetin, diacetate
	Phytol
	Stigmasterol

In silico analysis of selected compounds

All the ligands were docked against different proteins. The binding energies of ligands of *C. quadrangularis* (Table 5), *C. odorata* (Table 6) and standard drugs (Table 7) obtained from the RMSD table are tabulated. The binding energies of 1-tridecene, 13-docosenamide, (z)-, behenic alcohol, diphenyl sulfone, neophytadiene, n-nonadecanol-1, octacosane, 1-iodo-, phytol, and squalene of EACQ towards interleukin 6 of human and mice were -3.9, -5.1, -4.5, -5.6, -5.0, -4.3, -3.9, -5.1 and -6.5 Kcal/mol respectively and for interleukin 6 of rat, it was -5.1, -6.3, -5.7, -6.9, -7.1, -5.9, -6.0, -7.0, and -7.1 respectively. Same compounds showed a binding energy of -4.8, -5.8, -5.2, -6.0, -6.0, -5.3, -4.5, -6.1 and -5.6 Kcal/mol towards vascular endothelial factor B and -5.6, -6.6, -6.2, -7.2, -6.9, -6.1, -5.6, -7.3 and -8.5 Kcal/mol towards penicillin binding protein 2a respectively.

Table 5. Binding energy of different ligands of *C. quadrangularis*

NO.	LIGANDS	1N26	P20607	2C7W	1VQQ
1	1-Tridecene	-3.9	-5.1	-4.8	-5.6
2	13-Docosenamide, (Z)-	-5.1	-6.3	-5.8	-6.6
3	Behenic alcohol	-4.5	-5.7	-5.2	-6.2
4	Diphenyl sulfone	-5.6	-6.9	-6.0	-7.2
5	Neophytadiene	-5.0	-7.1	-6.0	-6.9
6	n-Nonadecanol-1	-4.3	-5.9	-5.3	-6.1
7	Octacosane, 1-iodo-	-3.9	-6.0	-4.5	-5.6
8	Phytol	-5.1	-7.0	-6.1	-7.3
9	Squalene	-6.5	-7.1	-5.6	-8.5

Table 6. Binding energy of different ligands of *C. odorata*

No.	LIGANDS	1N26	P20607	2C7W	1VQQ
1	Gamma sitosterol	-8.0	-9.6	-8.5	-10.7
2	2-(3,4-Dimethyloxyphenyl)-2,3-dihydro-5,7-dihydroxy-4H-1-benzopyran-4-one	-6.7	-8.7	-7.3	-9.6
3	2'-Hydroxy-4,4',5',6'-tetramethoxychalcone	-5.8	-7.6	-6.6	-7.9
4	3',4',5,6,7-Pentamethoxyflavanone	-6.6	-8.1	-7.0	-8.1
5	4H-1-Benzopyran-4-one, 5,6,7-trimethoxy-2-(4-methoxyphenyl)-	-6.3	-8.0	-6.8	-8.4
6	5,6,7,4'-Tetramethoxyflavanone	-6.4	-7.9	-6.8	-8.3
7	Aromandendrene	-6.9	-8.6	-7.1	-8.4
8	Epilupeol	-11	-11.5	-10.8	-12.7
9	Isosakuranetin, diacetate	-6.9	-8.6	-7.2	-9.5
10	Phytol	-4.4	-7.0	-6.1	-7.3
11	Stigmasterol	-8.2	-10.1	-8.9	-11.4

Gamma sitosterol, 2-(3,4-dimethyloxyphenyl)-2,3-dihydro-5,7-dihydroxy-4h-1-benzopyran-4-one, 2'-hydroxy -4,4',5',6'-tetramethoxychalcone, 3',4',5,6,7-pentamethoxy flavanone, 4h-1-benzopyran-4-one, 5,6,7-trimethoxy-2- (4-methoxyphenyl), 5,6,7,4'-tetramethoxyflavanone, aromandendrene, epilupeol, isosakuranetin, diacetate, phytol and stigmasterol from EECO showed binding energies of -8.0, -6.7, -5.8, -6.6, -6.3, -6.4, -6.9, -11, -6.9, -4.4 and -8.2 Kcal/mol and -9.6, -8.7, -7.6, -8.1, -8.0, -7.9, -8.6, -11.5, -8.6, -7.0 and -10.1 Kcal/mol respectively towards interleukin 6 of human and mice and rat. Binding energies of -8.5, -7.3, -6.6, -7.0, -6.8, -6.8, -7.1, -10.8, -7.2, -6.1 and -8.9 Kcal/mol were shown towards vascular endothelial growth factor B whereas -10.7, -9.6, -7.9, -8.1, -8.4, -8.3, -8.4, -12.7, -9.7, -7.3 and -11.4 Kcal/mol binding energies were shown towards penicillin binding protein 2a.

Table 7. Binding energy of standards

NO.	LIGANDS	1N26	P20607	2C7W	1VQQ
1	Indomethacin	-5.9	-6.1	-6.1	-7.2
2	Allantoin	-4.6	-5.2	-5.1	-6.3
3	Ceftriaxone	-6.3	-7.7	-6.6	-6.9

Among the various phytocompounds, the present study showed that squalene of EACQ and epilupeol of EECO had least binding energy towards different proteins of antimicrobial resistance and wound healing. Docked images of different proteins with ligands of *C. quadrangularis* and *C. odorata* are shown (Figure 7- 15).

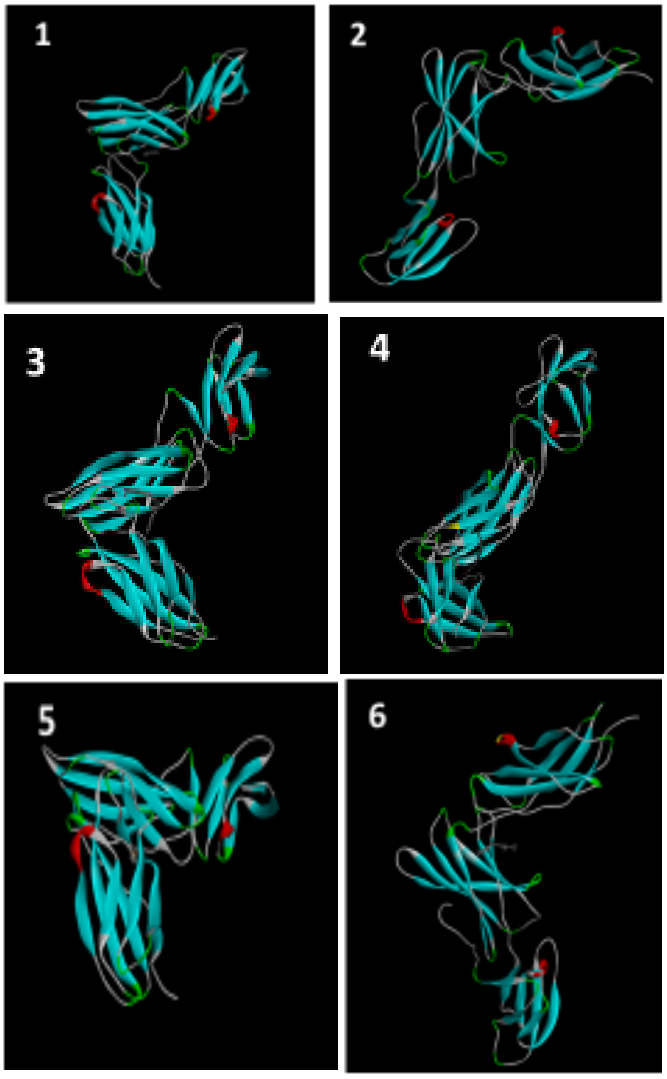

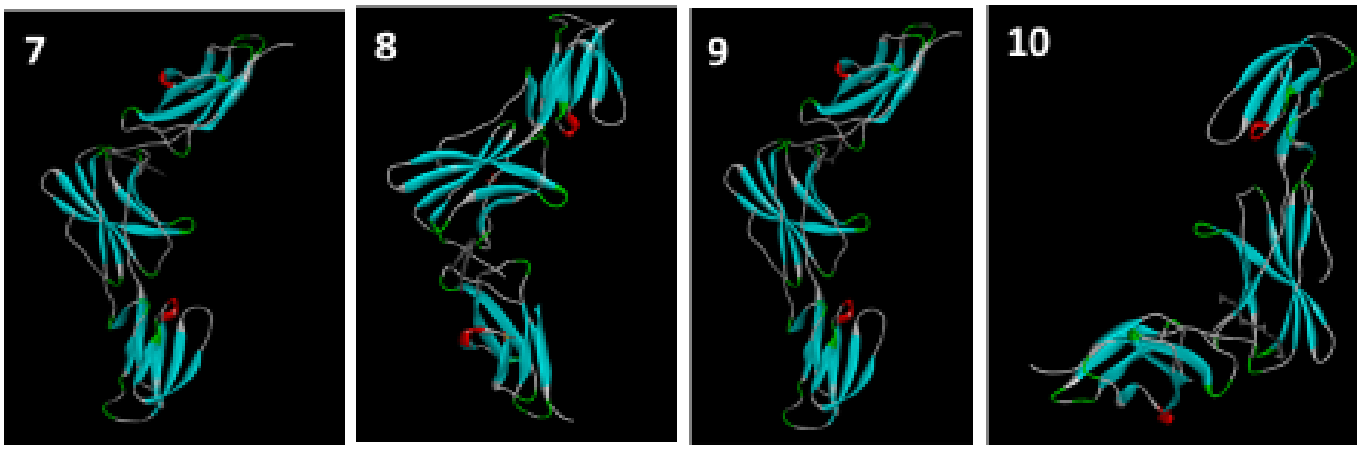

Fig. 7. Ligands of *C. quadrangularis* (**1**- 1-Tridecene, **2**- 4,4'-((p-Phenylene) diisopropylidene)diphenol, **3**- 13-Docosenamide, (Z)-, **4**- Behenic alcohol, **5**- Diphenyl sulfone, **6**- Neophytadiene, **7**- n-Nonadecanol-1, **8**- Octacosane, 1-iodo-, **9**- Phytol and **10**- Squalene) docked against protein IL6 (human and mice).

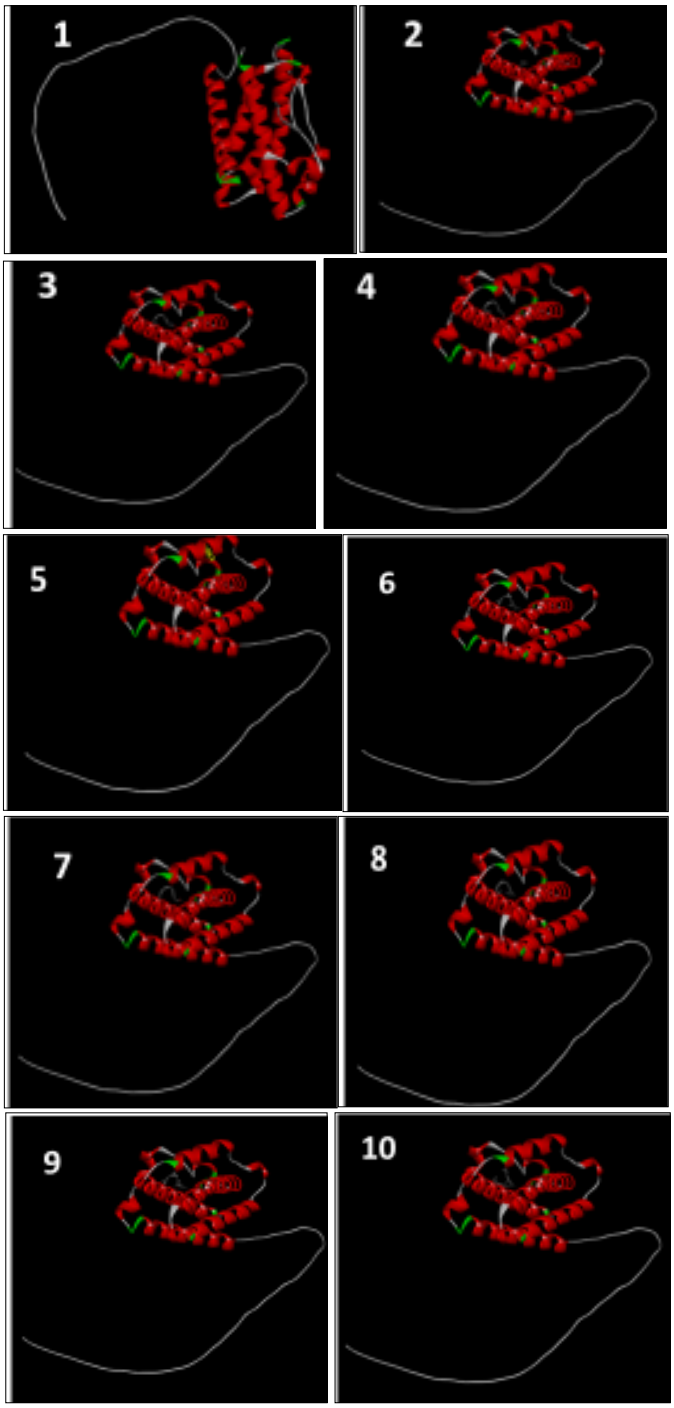

Fig. 8. Ligands of *C. quadrangularis* (**1**- 1-Tridecene, **2**- 4,4'-((p-Phenylene) diisopropylidene)diphenol, **3**- 13-Docosenamide, (Z)-, **4**- Behenic alcohol, **5**- Diphenyl sulfone, **6**- Neophytadiene, **7**- n-Nonadecanol-1, **8**- Octacosane, 1-iodo-, **9**- Phytol and **10**- Squalene) docked against protein IL6 (rat)

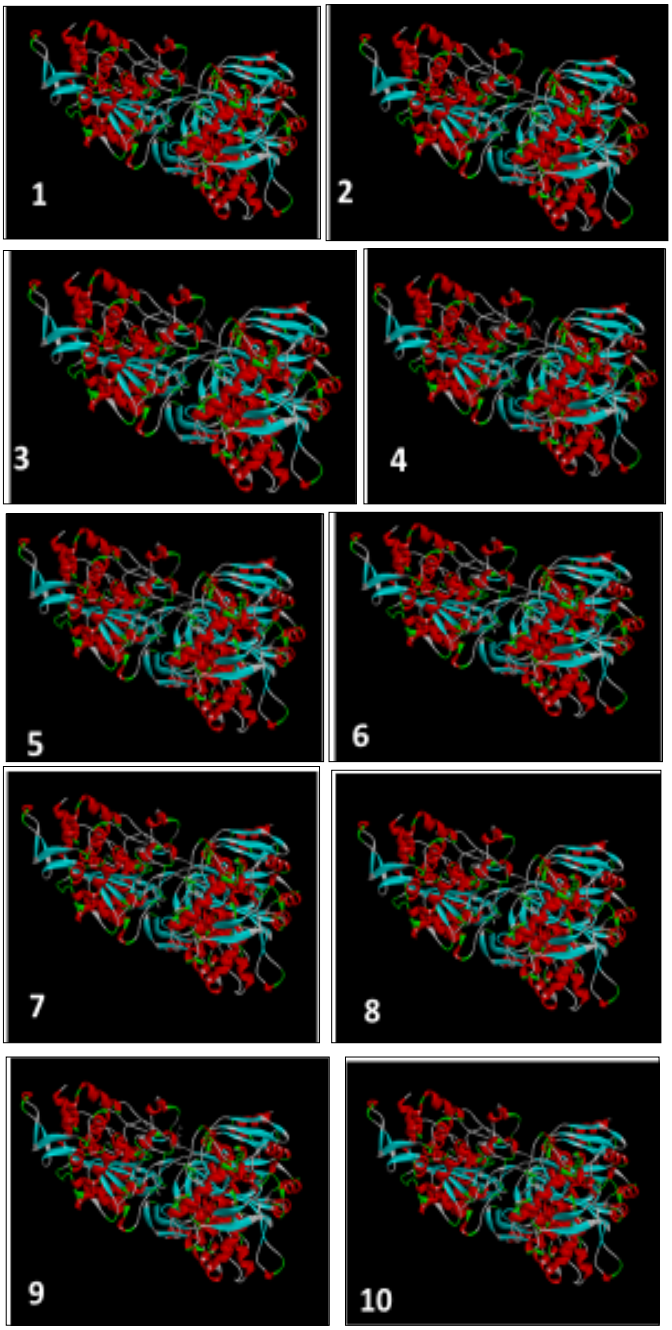

Fig. 9. Ligands of *C. quadrangularis* (**1**- 1-Tridecene, **2**- 4,4'-((p-Phenylene) diisopropylidene)diphenol, **3**- 13-Docosenamide, (Z)-, **4**- Behenic alcohol, **5**- Diphenyl sulfone, **6**- Neophytadiene, **7**- n-Nonadecanol-1, **8**- Octacosane, 1-iodo-, **9**- Phytol and **10**- Squalene) docked against protein PBP 2a (human, rat and mice)

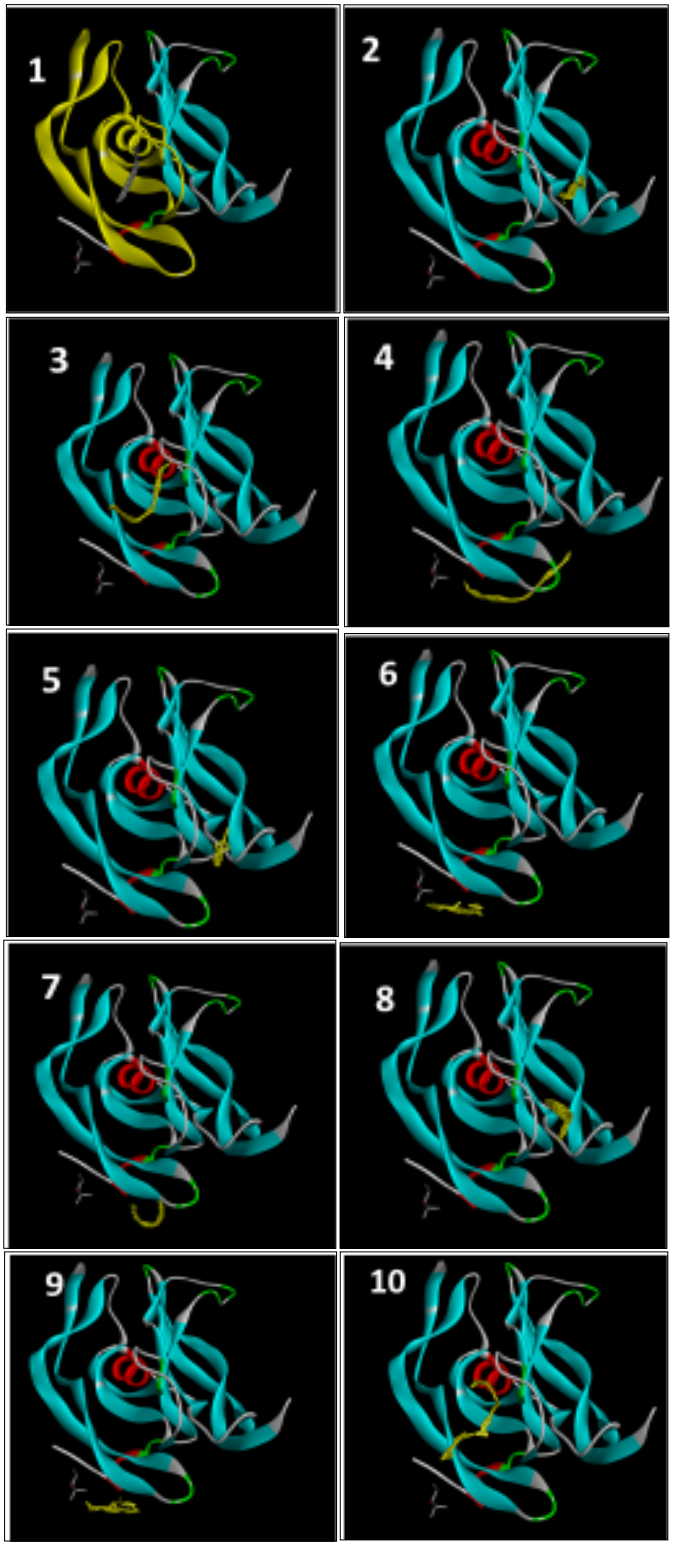

Fig. 10. Ligands of *C. quadrangularis* (**1**- 1-Tridecene, **2**- 4,4'-((p-Phenylene) diisopropylidene)diphenol, **3**- 13-Docosenamide, (Z)-, **4**- Behenic alcohol, **5**- Diphenyl sulfone, **6**- Neophytadiene, **7**- n-Nonadecanol-1, **8**- Octacosane, 1-iodo-, **9**- Phytol and **10**- Squalene) docked against protein VEGF (human, rat and mice)

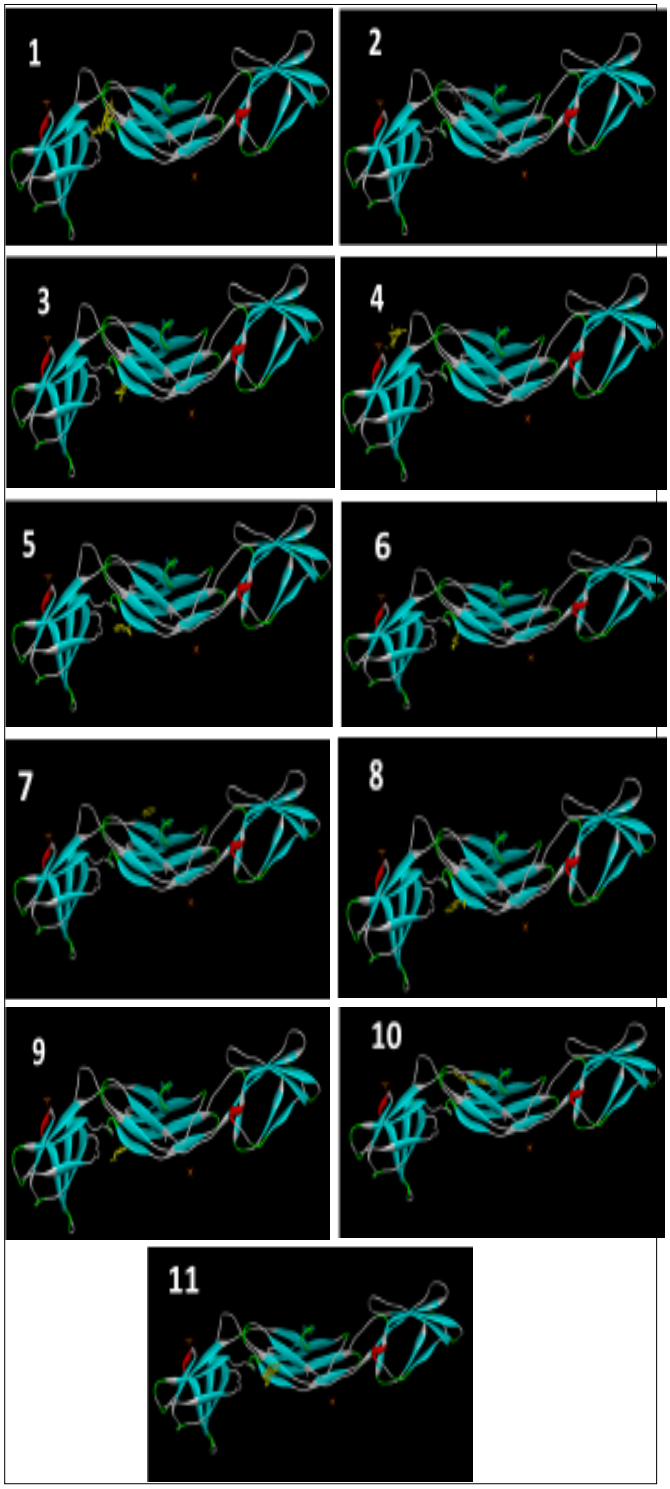

Fig. 11. Ligands of *C. odorata* (**1**- Gamma sitosterol, **2**- 2-(3,4-Dimethyloxy phenyl)-2,3-dihydro-5,7-dihydroxy-4H-1-benzopyran-4-one, **3**- 2'-Hydroxy-4,4',5',6'-tetramethoxychalcone, **4**- 3',4',5,6,7-Pentamethoxyflavanone, **5**- 4H -1-Benzopyran-4-one, 5,6,7-trimethoxy-2-(4-methoxyphenyl), **6**- 5,6,7,4'-Tetramethoxyflavanone, **7**- Aromandendrene, **8**- Epilupeol, **9**- Isosakuranetin, diacetate, **10**- Phytol, **11**- Stigmasterol) docked against protein IL6 (human and mice)

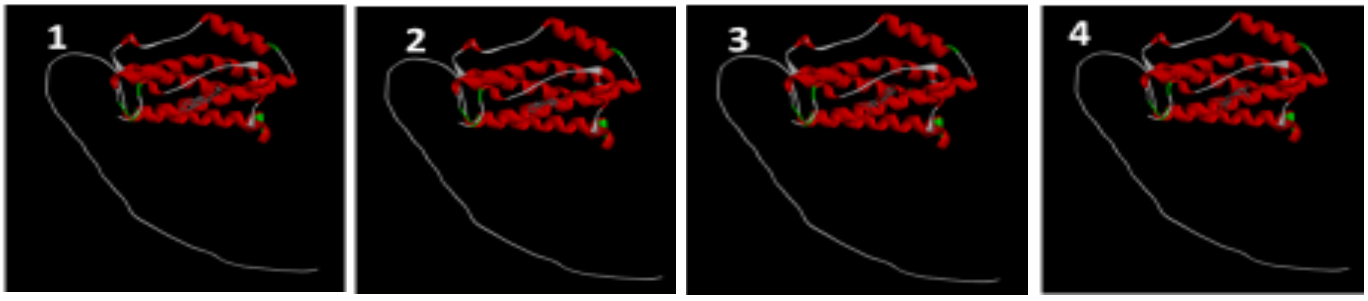

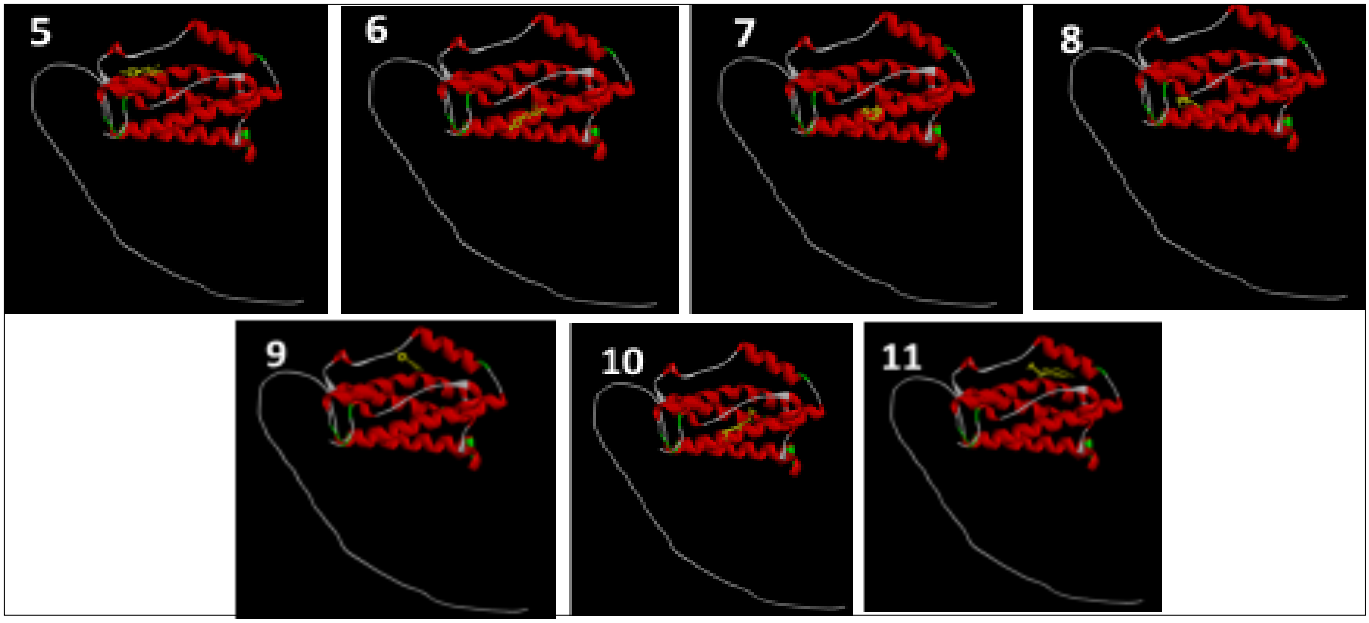

Fig. 12. Ligands of *C. odorata* (**1**- Gamma sitosterol, **2**- 2-(3,4-Dimethyloxyphenyl)-2,3-dihydro-5,7-dihydroxy-4H-1-benzopyran-4-one, **3**- 2'-Hydroxy-4,4',5',6'-tetramethoxychalcone, **4**- 3',4',5,6,7-Pentamethoxyflavanone, **5**- 4H-1-Benzopyran-4-one, 5,6,7-trimethoxy-2-(4-methoxyphenyl), **6**- 5,6,7,4'-Tetramethoxy- flavanone, **7**- Aromandendrene, **8**- Epilupeol, **9**- Isosakuranetin, diacetate, **10**- Phytol, **11**- Stigmasterol) docked against protein IL6 (rat)

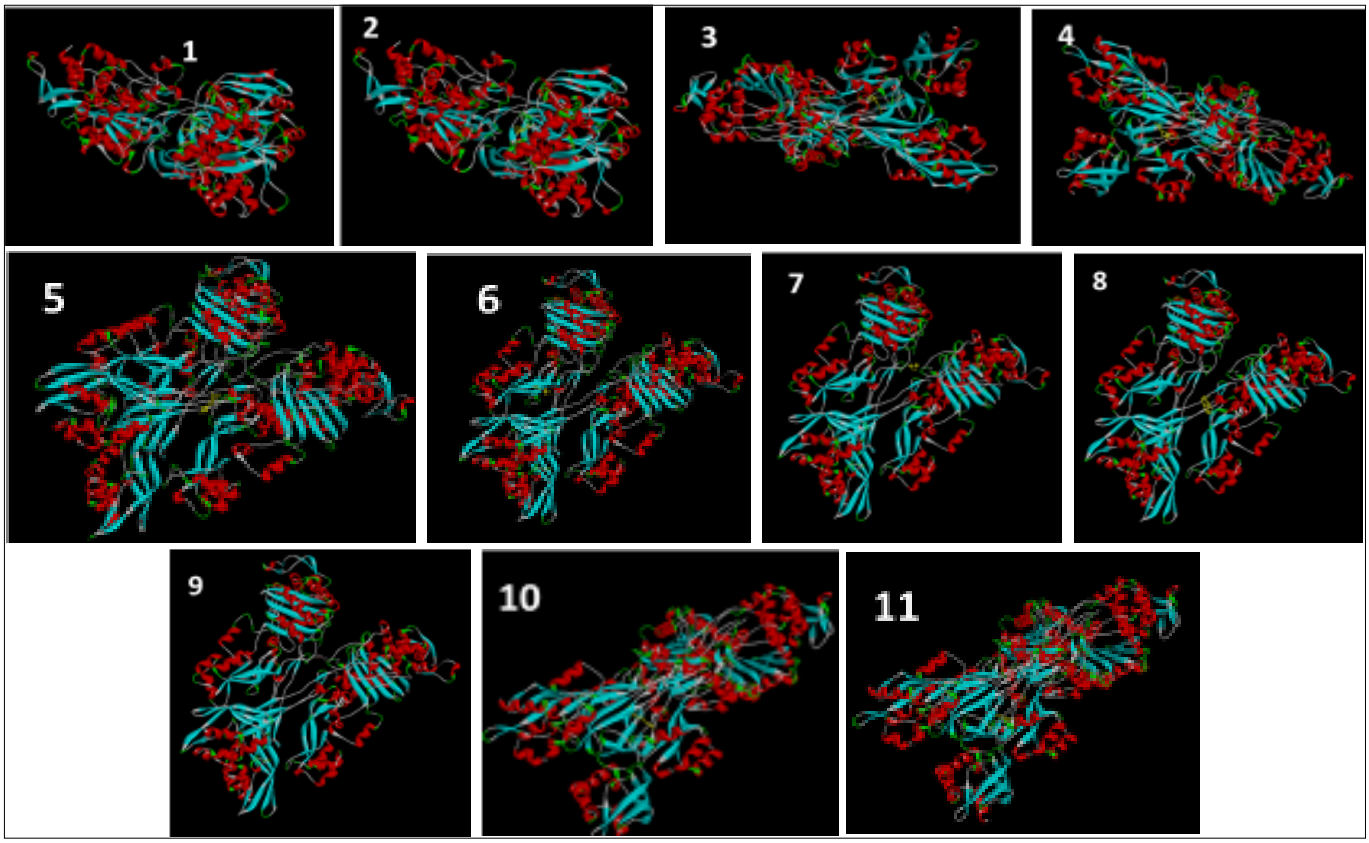

Fig. 13. Ligands of *C. odorata* (**1**- Gamma sitosterol, **2**- 2-(3,4-Dimethyloxyphenyl)-2,3-dihydro-5,7-dihydroxy-4H-1-benzopyran-4-one, **3**- 2'-Hydroxy-4,4',5',6'-tetramethoxychalcone, **4**- 3',4',5,6,7-Pentamethoxyflavanone, **5**- 4H-1-Benzopyran-4-one, 5,6,7-trimethoxy-2-(4-methoxyphenyl), **6**- 5,6,7,4'-Tetramethoxy- flavanone, **7**- Aromandendrene, **8**- Epilupeol, **9**- Isosakuranetin, diacetate, **10**- Phytol, **11**- Stigmasterol) docked against protein PBP 2a (human, rat and mice)

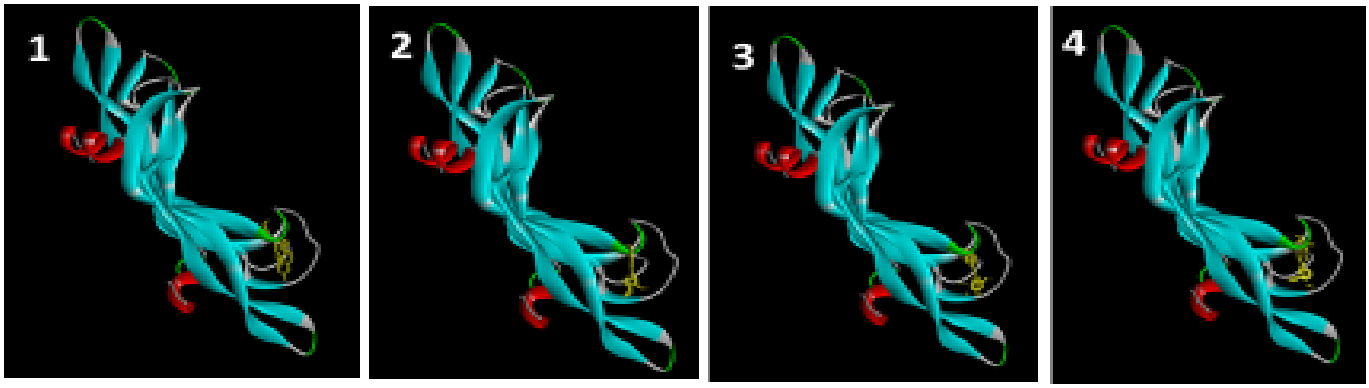

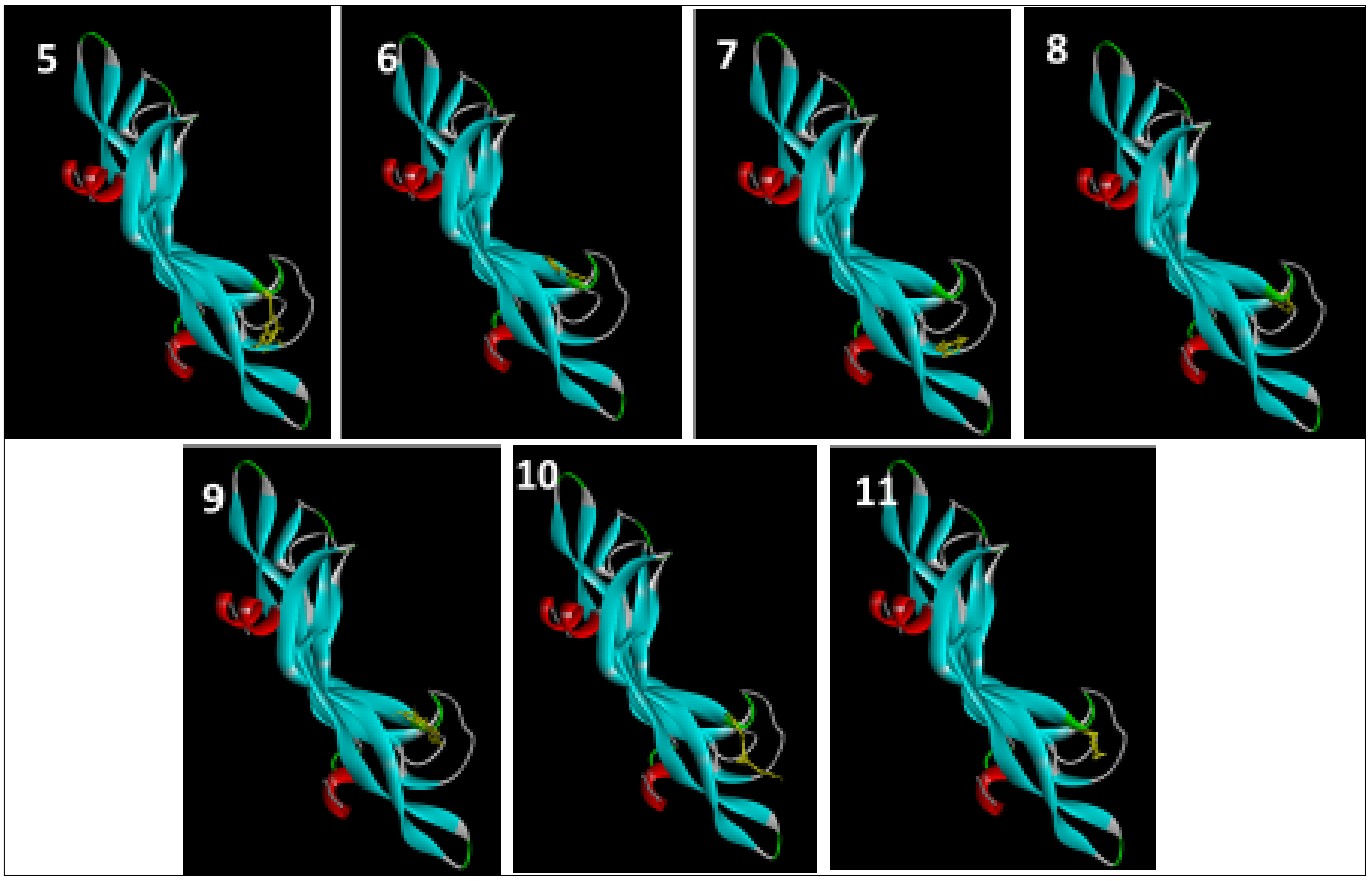

Fig. 14. Ligands of *C. odorata* (**1**- Gamma sitosterol, **2**- 2-(3,4-Dimethyloxyphenyl)-2,3-dihydro-5,7-dihydroxy-4H-1-benzopyran-4-one, **3**- 2'-Hydroxy-4,4',5',6'-tetramethoxychalcone, **4**- 3',4',5,6,7-Pentamethoxyflavanone, **5**- 4H-1-Benzopyran-4-one, 5,6,7-trimethoxy-2-(4-methoxyphenyl), **6**- 5,6,7,4'-Tetramethoxy- flavanone, **7**- Aromandendrene, **8**- Epilupeol, **9**- Isosakuranetin, diacetate, **10**- Phytol, **11**- Stigmasterol) docked against protein VEGF (human, rat and mice)

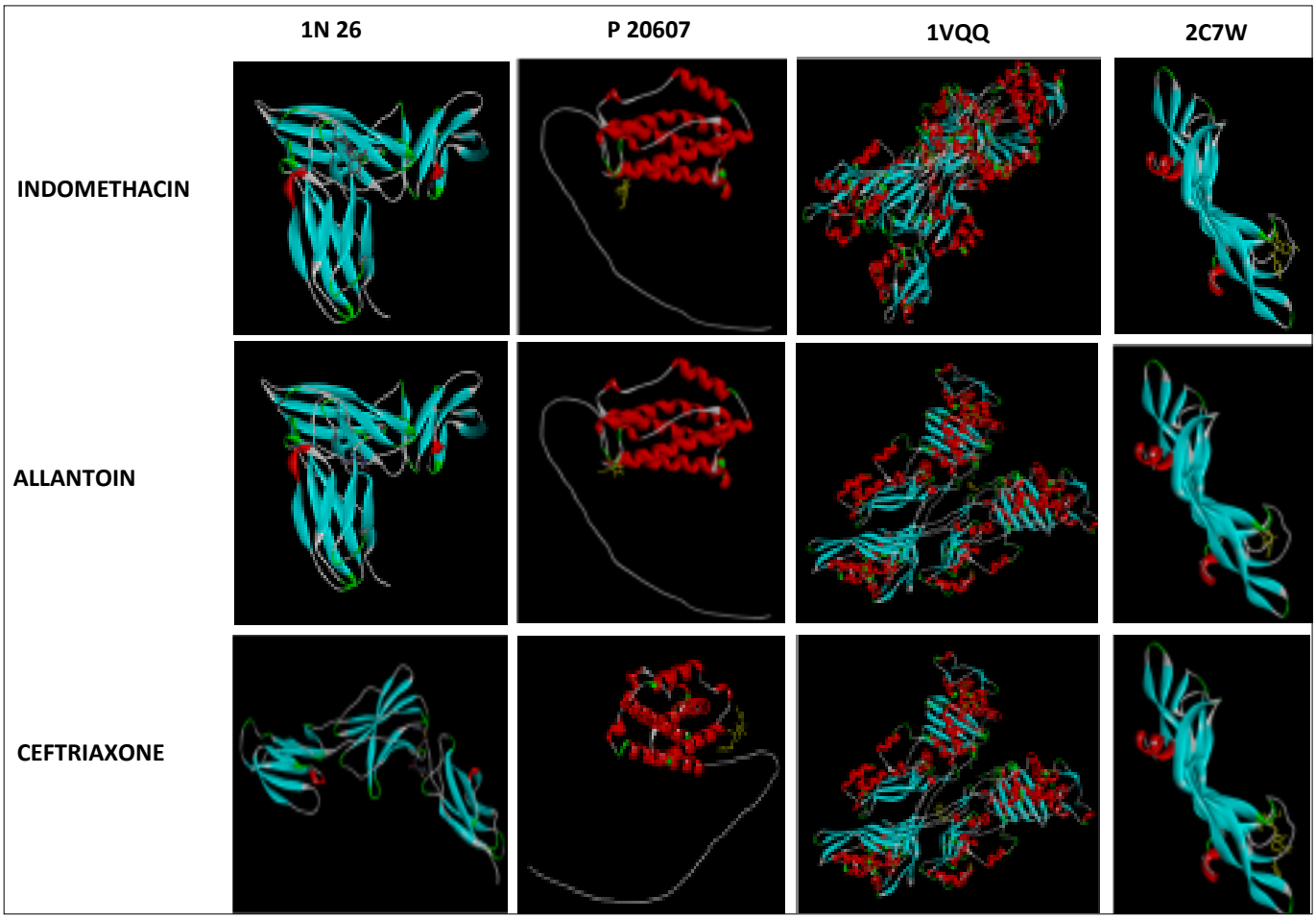

Fig. 15. Standard drugs docked against proteins of MRSA infected wound healing

Discussion

GC- MS analysis of EACQ and EECO

Gas chromatography -mass spectrometric analysis of EACQ revealed the presence of 24 compounds while EECO showed 37 compounds. In a previous study, GC-MS analysis of *C. quadrangularis* stem reported the presence of eugenol, n-hexadecanoic acid, 1,2-benzenedicarboxylic acid, diisooctyl ester and 2,4-bis(1-phenylethyl) – phenol (7). In the GC-MS analysis of essential oils from *C. odorata*, presence of α-pinene, β-pinene, germacrene D, limonene, δ-elemene and geijerene were detected (8). The GC-MS analysis of essential oils obtained from the aerial parts of *C. odorata* revealed geijerene, α-copaene, caryophyllene, 3-carene, cadinene, cyclohexane, 1-methylene-4-(1-methylethenyl)-, elemol and τ-muurolol as the major components (9). In the present study, the reported compounds were different from those cited. This difference in the various phytocompounds might be attributed to factors such as climate, soil, season and difference in the solvents used for extraction (10).

In silico analysis of compounds

In the process of wound healing, the transition from pro-inflammatory to a reparative microenvironment has to be precisely controlled (11). A crucial regulator of the inflammatory and reparative process is IL-6 (12). Interleukin-6 helps in leukocyte differentiation, endothelial activation, keratinocyte proliferation, and fibroblast proliferation (13). Hence *in silico* docking studies of various ligands of EACQ and EECO were conducted against the receptor IL-6 of human, mice and rat. The *in silico* docking results of ligands of EACQ revealed that all the compounds except 1-tridecene showed good binding affinity to IL-6 and the maximum binding affinity was exhibited by squalene whereas all the compounds of EECO exhibited good binding affinity for IL-6 with maximum binding affinity for epilupeol. This study first reports the interaction of IL-6 with epilupeol as there are no reported studies about the interaction of IL-6 with epilupeol.

One of the key proteins involved in antimicrobial resistance is pencillin binding protein (PBP)2a which confers resistance to beta lactam antibiotics in *S. aureus* (14). Compounds that inhibit PBP2a offer promising treatment against antibiotic resistant infections. In the present study, squalene from EACQ and all the compounds of EECO showed good binding affinity for PBP2a, comparable to the standard drug, ceftriaxone. Thus it could be inferred that EECO offered better inhibition of antimicrobial resistance than EACQ. Thus EECO could offer better promising treatment against MRSA infection. Among the various compounds of EACQ and EECO, squalene and epilupeol showed good binding affinity towards PBP2a. This study first reports the inhibition of antimicrobial resistance of these compounds against MRSA as there are no reported works.

Vascular endothelial growth factor (VEGF)-B is involved in the maintenance of newly formed blood vessels in pathological conditions and it indirectly influence the vascular growth by influencing VEGF-A action (15). In the present study, five compounds of EACQ and all the 11 compounds of EECO was found to have a good binding affinity when compared to the standard drug, allantoin. As observed for IL-6 and PBP2a, squalene and epilupeol showed maximum binding affinity for VEGF-B also. As there are no reported works related to the binding affinity of these compounds against VEGF-B, this study first reports this interaction. Thus it could be assumed that EECO could offer better maintenance of newly formed blood vessels in MRSA infected wound conditions and promote wound healing.

In the present study, different phytocompounds showed better affinity towards proteins of antimicrobial resistance and wound healing as compared to standard ligands used. Squalene is a bioactive triterpene that occurs naturally plays a key role in the process of making sterols and has good wound healing activity (16). Squalene promotes wound healing by increasing macrophage response in inflammation. Therefore, squalene could be useful at the resolution stage of wound healing (17). This is in accordance with the results of the present study, where binding energies of squalene with IL6 of and VEGF-B are -6.5 (human, mice), -7.1(rat) and -5.6 (human, mice and rat) Kcal/mol indicating good affinity towards proteins of wound healing.

Phytol showed a binding energy of -7.3 Kcal/mol towards PBP 2a indicating good affinity. Phytol showed a biphasic effect and appeared to have both bacterial growth-inhibitory and growth-accelerating effects, and the net effect of each depended on its concentration (18). Methanolic extract of *Phlomis russeliana* exhibited *in vitro* and *in vivo* wound healing activity which was attributed to the presence of phytol and 1-heptadecanoic acid as active constituents (19). Thus it could be assumed that EACQ and EECO could be effective in antibiotic resistant infectious wound.

Gamma sitosterol showed lower binding energies compared to standards towards proteins of wound healing and penicillin resistance. Gamma sitosterol is shown to inhibit matrix metalloproteinase -1 (MMP-1), reduce collagen breakdown, and promote the synthesis of collagen in human keratinocytes (6). Moreover, they promote keratinocyte migration through the reduction of oxidative stress that effectively accelerates the healing process (20). Hemostatic and wound healing properties of *C. odorata* could be attributed to the presence of major phytoconsti- tuents scutellarin and stigmasterol (8). This corroborates with present study where stigmasterol from *C. odorata* showed binding energies of higher negativity as compared to standard drugs. No data is available on activity of other compounds on antibiotic resistant infectious wound healing.

Conclusion

Most phytoconstituents of plants *C. quadrangularis* exhibit higher negativity in binding energy when compared to standard compounds. In terms of affinity towards protein PBP 2a, compounds squalene and phytol of *C. quadrangularis* showed more affinity. Most of the constituents showed higher affinity towards VEGF and IL6 when compared to standards in

which squalene being the highest. In case of phytoconstituents of *C. odorata,* epilupeol showed most affinity towards the proteins, followed by stigmasterol, gamma sitosterol and 2-(3,4-Dimethyloxyphenyl)-2,3-dihydro-5,7-dihydroxy-4H-1-benzopyran-4-one. To summarize, both plants had phytoconstituents that have good affinity towards proteins of antibacterial resistance and wound healing. Among the plants, *C. odorata* showed higher affinity towards these proteins when compared *C. quadrangularis*. Further *in vitro* and *in vivo* studies are required to confirm the antibacterial and wound healing potential of these phytocompounds.

Acknowledgements

The authors acknowledge the financial assistance provided by Kerala Veterinary and Animal Sciences University as M.V.Sc. Research grant to the first author with grant number KVASU/2021/58/MVM/VPT as per order no. KVASU/DAR/Acad/A1/30274/2023 dt. 01/02/2023. The assistance provided by Dr. Devu B. Nair, Dr. Jida M.D., Dr. Divya Rajaselvi and Dr. Arundhathi S. Nair is duly acknowledged.

Authors contributions

ASS carried out the research work. BJK conceptualized and designed the experiment. PMK assisted in research work, article preparation and corrections. HSVJ participated in the docking studies.

Compliance with ethical standards

Conflict of interest: Authors do not have any conflict of interests to declare.

Ethical issues: None.

References

1. Guo SA, DiPietro LA. Factors affecting wound healing. J Dent Res.2010;89(3):pp.219-29. https://doi.org/10.1177/0022034509359125
2. Hiramatsu K, Cui L, Kuroda M, Ito T. The emergence and evolution of methicillin-resistant *Staphylococcus aureus*. Trends Microbiol. 2001;9(10):pp.486-93. https://doi.org/10.1016/S0966-842X(01)02175-8
3. Mishra G, Srivastava S, Nagori BP. Pharmacological and therapeutic activity of *Cissus quadrangularis*: An overview. Int J Pharmtech Res. 2010;2(2):pp.1298-310.
4. Zachariades C, Day M, Muniappan R, Reddy GVP. *Chromolaena odorata* (L.) king and robinson (Asteraceae). Biological control of tropical weeds using arthropods. Cambridge University Press, Cambridge. 2009;pp.130-62. https://doi.org/10.1017/CBO9780511576348.008
5. Murthy KNC, Vanitha A, Swamy MM, Ravishankar GA. Antioxidant and antimicrobial activity of *Cissus quadrangularis* L. J Med. Food. 2003;6:99-105. https://doi.org/10.1089/109662003322233495
6. Thophon SHS, Waranusantigul P, Kangwanrangsan N, Krajangsang S. Antimicrobial activity of *Chromolaena odorata* extracts against bacterial human skin infections. Mod Appl Sci. 2016;10p. https://doi.org/10.5539/mas.v10n2p159
7. Sathyaprabha G, Kumaravel S, Ruffina D, Praveenkumar P. A comparative study on antioxidant, proximate analysis, antimicrobial activity and phytochemical analysis of *Aloe vera* and *Cissus quadrangularis* by GC-MS. J Pharm Res. 2010;3:2970-73.
8. Owolabi MS, Ogundajo A, Yusuf KO, Lajide L, Villanueva HE, Tuten JA, Setzer WN. Chemical composition and bioactivity of the essential oil of *Chromolaena odorata* from Nigeria. Rec Nat Prod. 2010;4:72-79.
9. Gogoi R, Sarma N, Begum T, Pandey SK, Lal M. North-East Indian *Chromolaena odorata* (L. King Robinson) aerial part essential oil chemical composition, pharmacological activities-neurodegenerative inhibitory and toxicity study. J Essent Oil-Bear Plants. 2020;23:1173-91. https://doi.org/10.1080/0972060X.2020.1867009
10. Kumar S, Yadav A, Yadav M, Yadav JP. Effect of climate change on phytochemical diversity, total phenolic content and *in vitro* antioxidant activity of *Aloe vera* (L.) Burm. f. BMC Res Notes. 2017;10:1-12. https://doi.org/10.1186/s13104-017-2385-3
11. Johnson BZ, Stevenson AW, Prêle CM, Fear MW, Wood FM. The role of IL-6 in skin fibrosis and cutaneous wound healing. Biomedicines. 2020;8(5):p.101. https://doi.org/10.3390/biomedicines8050101
12. Lin ZQ, Kondo T, Ishida Y, Takayasu T, Mukaida N. Essential involvement of IL-6 in the skin wound-healing process as evidenced by delayed wound healing in IL-6-deficient mice. J Leukoc Biol. 2003;73:713-21. https://doi.org/10.1189/jlb.0802397
13. Weissenbach M, Clahsen T, Weber C, Spitzer D, Wirth D, Vestweber D, Heinrich PC, Schaper F. Interleukin-6 is a direct mediator of T cell migration. Eur J Immunol. 2004;34:2895-906. https://doi.org/10.1002/eji.200425237
14. Peacock SJ, Paterson GK. Mechanisms of methicillin resistance in *Staphylococcus aureus*. Annual Review of Biochemistry. 2015;84:pp.577-601. https://doi.org/10.1146/annurev-biochem-060614-034516
15. Lal N, Puri K, Rodrigues B. Vascular endothelial growth factor B and its signaling. Front Cardiovasc Med. 2018;5:39. https://doi.org/10.3389/fcvm.2018.00039
16. Aslam MS, Kim YJ, Linchao Q *et al*. A bio-therapeutically squalene: Case review for T&CM students as a wound-healing compound. In Cases on Teaching Pharmacology to Complementary and Alternative Medicine Students. 2023;p. 53-65. https://doi.org/10.4018/978-1-6684-7828-8.ch004
17. Sánchez-Quesada C, López-Biedma A, Toledo E, Gaforio JJ *et al*. Squalene stimulates a key innate immune cell to foster wound healing and tissue repair. Evid Based Complementary Altern Med. 2018. https://doi.org/10.1155/2018/9473094
18. Inoue Y, Hada T, Shiraishi A, Hirose K, Hamashima H, Kobayashi S *et al*. Biphasic effects of geranylgeraniol, teprenone and phytol on the growth of *Staphylococcus aureus*. Antimicrob Agents Chemother. 2005;49(5):1770-74. https://doi.org/10.1128/AAC.49.5.1770-1774.2005
19. Okur ME, Karadağ AE, Üstündağ Okur N, Özhan Y, Sipahi H, Ayla Ş, Daylan B, Demirci B, Demirci F *et al. In vivo* wound healing and *in vitro* anti-inflammatory activity evaluation of *Phlomis russeliana* extract gel formulations. Molecules. 2020;25(11):2695. https://doi.org/10.3390/molecules25112695
20. Poljšak N, Kočevar Glavač N. *Tilia* Sp. seed oil—composition, antioxidant activity and potential use. Appl Sci. 2021;11:4932. https://doi.org/10.3390/app11114932
21. Hernandez GR, Hernandez Garcia DY, Sanchez ML *et al*. Healing cream *Tournefortia hirsutissima* L. Med Aromat Plants. 2017;6:4-6. https://doi.org/10.4172/2167-0412.1000295
22. Pandith H, Zhang X, Liggett J, Min KW, Gritsanapan W, Baek SJ. Hemostatic and wound healing properties of *Chromolaena odorata* leaf extract. Int Sch Res Notices. 2013. https://doi.org/10.1155/2013/168269